

Aromaticity of α -Oligothiophenes and Equivalent Oligothienoacenes

Inmaculada García Cuesta,*† Juan Aragó,† Enrique Ortí,† and Paolo Lazzaretti‡

*Instituto de Ciencia Molecular, Universidad de Valencia, P.O. Box 22085,
E-46071 Valencia, Spain, and Dipartimento di Chimica, Università degli Studi di
Modena e Reggio Emilia, via Campi 183, 41100 Modena, Italy*

Received March 17, 2009

Abstract: The aromaticity and the degree of π -electronic delocalization have been theoretically investigated for α,α' -linked oligothiophenes containing three and five rings and for their fused analogs oligothienoacenes. By computing magnetic susceptibilities and ^1H NMR shieldings as well as current density maps, it is found that the fused oligomers are more aromatic than the corresponding nonfused partners. The increase of aromaticity with the size of the oligomer—even in the case of quinoidal forms—is also proven. The π -currents induced by an external magnetic field show that oligothienoacenes behave as single cycles since they present an intense diamagnetic current flowing around the whole molecular perimeter. In contrast, nonfused α -oligothiophenes exhibit diamagnetic currents localized over each thiophene ring. For the quinoidal oligomers, local diamagnetic π vortices appear around CC double bonds, indicating that the π electrons are rather localized as in conjugated, nonaromatic polyenes. For quinoidal nonathienoacene, it is however found that the electronic circulation around the ethylenic bonds tends to delocalize all over the carbon skeleton, indicating a more effective π -conjugation and some aromatic character.

1. Introduction

Since Faraday's discovery of benzene almost 200 years ago, the features associated with aromaticity have fascinated chemists.¹ Even at present, when thousands of aromatic compounds are known, research on aromaticity and aromatic compounds is still in progress. In particular, one of the areas in which aromaticity plays an essential role is the field of electroactive organic materials for molecular electronics as, for instance, small-molecule semiconductors and conducting polymers.^{2,3} The achievement of the electric and/or optical response always involves structural changes in the molecules constituting the material that imply a gain or a loss in aromaticity. Organic electroactive materials are obtained by chemical or electrochemical synthesis, and their properties can be easily tuned by adding functional groups to their π -conjugated structure.^{4–8} It is also important to recall their

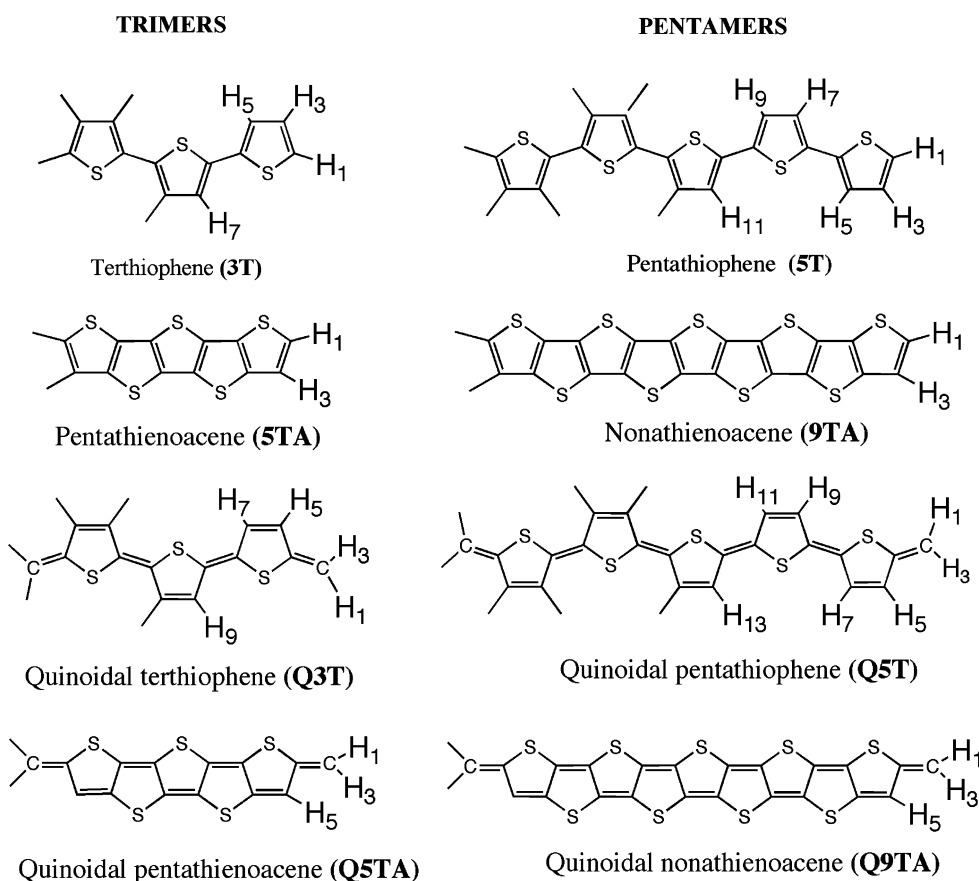
exceptional stability under different environments. Therefore, it is not surprising that there exists an enormous effort in developing technological applications of these materials such as organic light-emitting diodes (OLEDs), organic field-effect transistors (OFETs), flexible and large area displays, bio-sensors, lightweight photovoltaic cells, or wearable electronic devices.^{9–14}

A vast majority of organic semiconductors and conducting polymers are built from aromatic systems such as benzene or thiophene and their fused derivatives used as monomer units. In these systems, the extended conjugation of the π electrons along the molecular skeleton determines the structural and electronic properties and accounts for their electric and optical behavior. Conducting polymers present two nondegenerate forms in their ground state, the *aromatic* and the *quinoidal* forms.^{15–17} Despite the fact that both forms are conjugated, the aromatic structure is usually preferred in the neutral state, and the quinoidal structure is only attained upon charge injection. Electronic delocalization along the π system is not enough to allow the material to become

* Corresponding author e-mail: garciain@uv.es.

† Universidad de Valencia.

‡ Università degli Studi di Modena e Reggio Emilia.

Scheme 1. Chemical Structures of the Oligomers Studied

conductor, and doping—oxidation/reduction of the material—is required to achieve the conducting state. Charge injection provokes the progressive quinoidization of the conjugated organic chain. The characteristics of the aromatic form strongly influence the possibilities of the material as conductor not only because they determine the easiness for oxidation or reduction but also because the electronic structure of the aromatic form is partly inherited by the quinoidal structure.¹⁶ In this sense, studying the aromaticity of conjugated oligomers is a relevant task because from this knowledge it is possible to provide useful information for the development of advanced semiconducting materials and at the same time to improve our understanding of aromaticity itself.

Among the different organic semiconducting materials, α -oligothiophenes (thiophene oligomers joined in α,α' positions by single bonds) represent a foremost group of molecules and have been widely employed as the active layers in organic electronic devices.^{6,7,11,12,18,19} α -Oligothiophenes show a good environmental stability and are easy to synthesize, and their electronic and solid-state properties can be modulated by introducing either donor or electron-withdrawing groups in their carbon skeleton.¹⁹ A main disadvantage of α -oligothiophenes is that they can deviate from planarity through torsion about the single inter-ring bonds thus decreasing the electron delocalization along the π -conjugated carbon backbone. In this context, oligothienoacenes (linearly fused thiophenes) are emerging as a promising new class of π -conjugated compounds that combine the rigid planarity and extended conjugation of acenes with the chemical stability of oligothiophenes.²⁰

Oligothienoacenes have been already implemented as the active layers in OFETs exhibiting an excellent field-effect performance with mobilities as high as $0.42 \text{ cm}^2 \text{ V}^{-1} \text{ s}^{-1}$.²¹ The structural and optical properties of penta- and heptathienoacene have been recently analyzed in comparison to those observed in α -oligothiophenes of identical conjugation length.²²

In this work, we perform a comparative study of the aromaticity of α -oligothiophenes with three (terthiophene, **3T**) and five (pentathiophene, **5T**) rings and of their oligothienoacene analogs of identical conjugation length (pentathienoacene, **5TA**, and nonathienoacene, **9TA**, respectively) in both aromatic and quinoidal forms (see Scheme 1). Our goal is to determine how the aromatic properties change with the following: i) the nonfused/fused character of the conjugated skeleton, ii) the number of monomeric units, and iii) the aromatic/quinoid nature of the carbon backbone. Quinoidal forms are built up by introducing end-capping methylene groups and will be denoted as **Q3T**, **Q5T**, **Q5TA**, and **Q9TA**, respectively. It should be stressed that the main structural difference between α -oligothiophenes and oligothienoacenes is the sulfur atoms that bridge the thiophene rings. For the sake of simplicity, we will refer the studied systems as trimers (**3T** and **5TA**) or pentamers (**5T** and **9TA**).

2. Computational Details

According to the ring-current model (RCM), the exposition of an aromatic cyclic system to an external magnetic field

Table 1. Magnetic Susceptibility Tensors in (cgs) ppm au^a via the CTOCD-DZ2 Method (Origin in the Center of Mass)^b

	xx	yy	zz (π)	Av	$\Delta\chi$
terthiophene (3T)	-1211.8	-1094.7	-2544.4 (-929.4)	-1616.9	-1391.2
pentathienoacene (5TA)	-1475.0	-1373.5	-3400.2 (-1576.0)	-2082.9	-1976.0
quinoidal terthiophene (Q3T)	-1440.8	-1199.5	-2116.3 (-376.7)	-1585.5	-796.1
quinoidal pentathienoacene (Q5TA)	-1749.8	-1503.4	-2441.8 (-505.5)	-1898.3	-815.2
pentathiophene (5T)	-2003.4	-1781.3	-4078.8 (-1450.5)	-2621.1	-2186.5
nonathienoacene (9TA)	-2534.5	-2327.2	-5755.3 (-2708.9)	-3539.0	-3324.4
quinoidal pentathiophene (Q5T)	-2265.8	-1879.7	-3374.3 (-633.5)	-2506.6	-1301.6
quinoidal nonathienoacene(Q9TA)	-2857.8	-2488.5	-4131.6 (-987.3)	-3157.9	-1458.5

^a The conversion factor from cgs au per molecule to cgs emu per mole is $a_0 N_A = 8.9238878 \times 10^{-2}$; further conversion to SI units is obtained by $1 \text{ JT}^{-2} = 0.1 \text{ cgs emu}$. ^b Contributions from π electrons to the zz component are given within parentheses. $\chi_{\text{Av}} = (\chi_{\text{xx}} + \chi_{\text{yy}} + \chi_{\text{zz}})/3$. Anisotropy $\Delta\chi = \chi_{\text{zz}} - 1/2(\chi_{\text{xx}} + \chi_{\text{yy}})$.

normal to the molecular plane induces π -electronic ring currents that produce an increase of the modulus of the magnetic susceptibility (χ) mainly due to an enlargement of its perpendicular component (χ_{zz}).^{1,23–28} At the same time, the π -currents diminish the perpendicular component of the nuclear magnetic shielding of the proton (σ_{zz}),^{1,26} which is normally known as downfield ¹H NMR chemical shift. It is important to emphasize that π -ring currents only modify the perpendicular component of the susceptibility and shielding tensors. Indeed, different causes contribute to determine the in-plane components, but none of them is related to the special mobility of the π -electrons and, therefore, to aromaticity. Consequently, criteria for diatropicity and aromaticity can only be based on the out-of-plane component of the magnetic tensors and not on the average (one-third of the trace) values. For planar molecules, the symmetry separation of σ and π orbitals is preserved, and, therefore, it is possible to evaluate only the contribution to those properties from π -electrons.

We have carried out a systematic analysis of the aromaticity of the studied compounds and, with this aim, determined their susceptibilities and NMR shieldings as well as the density maps of the current induced by the magnetic field. We have used the damped variant of a method allowing for continuous transformation of the origin of the current density-diamagnetic zero, CTOCD-DZ2,²⁹ inside the Coupled Hartree–Fock approach as implemented in the SYSMO suite of programs.³⁰ The selected basis sets were cc-pCVTZ for carbon^{31,32} and sulfur³³ and cc-pVTZ for hydrogen.³¹

Molecular geometries were optimized within the density functional theory (DFT) using the B3LYP functional³⁴ and the 6-31G** basis set³⁵ and imposing C_{2h} symmetry constraints. The Gaussian03 program³⁶ was used to this end. To test the influence of the molecular geometry on the magnetic properties, the geometry of pentathienoacene was also optimized using second-order Møller-Pleset (MP2) perturbation theory. Compared with the B3LYP/6-31G**-optimized geometry, MP2/6-31G** calculations predict slightly shorter single C–C (0.006–0.007 Å), C–S (0.013–0.017 Å), and C–H (0.003 Å) bonds and slightly longer double C=C bonds (0.008–0.009 Å). The variations on the magnetic properties due to these small geometrical changes are calculated to be rather unimportant since the average chemical shieldings vary in 0.07–0.10 ppm and their zz-component in 0.03–0.06 ppm. Changes in magnetic susceptibility are also small: 0.4% for χ_{Av} and 1.2% for χ_{zz} .

3. Results and Discussion

3.1. Magnetic Properties. The two trimers, terthiophene and pentathienoacene, have six carbon–carbon (CC) double bonds in their aromatic forms **3T** and **5TA** and seven CC double bonds in their quinoidal partners **Q3T** and **Q5TA**, but the fused oligomers (**5TA** and **Q5TA**) have two additional sulfur atoms and, therefore, a larger number of π electrons. A similar situation is found for the pentamers, for which the aromatic forms **5T** and **9TA** present one CC double bond less than the quinoidal structures **Q5T** and **Q9TA**—ten vs eleven—, while the four extra sulfur atoms in the fused counterparts provide them with an increased number of π -electrons.

All the considered aromatic systems are diatropic molecules, which means that they are able to sustain intense diamagnetic currents in the presence of an external magnetic field. The diatropic currents are however sensibly less intense for the quinoidal systems. The magnetic susceptibilities calculated for all of them, aromatic and quinoidal, are large and negative (see Table 1). The component normal to the molecular plane, χ_{zz} , is larger than the average in-plane components, making the susceptibility anisotropy, $\Delta\chi$, negative. The structural and electronic differences mentioned above are especially reflected by the degree of anisotropy. $\Delta\chi$ shows significantly larger values for the fused oligomers **5TA** (-1976.0 au) and **9TA** (-3324.4 au) than for their respective nonfused partners **3T** (-1391.2 au) and **5T** (-2186.5 au). Its absolute value increases with the length of the oligomer (57% in passing from **3T** to **5T**, 68% from **5TA** to **9TA**), which is mostly due to the larger contribution of the π electrons to the χ_{zz} component (56 and 72%, respectively). For the aromatic compounds, the value of χ_{zz} is more than twice (2.2 for **3T** and **5T**, 2.4 for **5TA** and **9TA**) the value of $1/2(\chi_{\text{xx}} + \chi_{\text{yy}})$, but the ratio between these values is significantly reduced in passing to the quinoidal compounds (1.6 for **Q3T** and **Q5T**, 1.5 for **Q5TA** and **Q9TA**). To compare with, let us recall that in benzene the perpendicular component is almost three times larger than the parallel components.²⁶

Obviously, going from aromatic to quinoidal oligomers implies a loss of aromaticity, which can be quantified in terms of the susceptibility anisotropy. There are two important issues to recall. First, the loss of aromaticity is larger the smaller is the oligomer. For the trimers it is of 43% (**3T**) and 59% (**5TA**), while for the pentamers is of 40% (**5T**) and 56% (**9TA**), i.e. some 3% lower, showing an increasing

Table 2. Proton Magnetic Shieldings of Oligothiophenes and Oligothienoacenes in ppm via the CTOCD-DZ2 Method^b

	xx	yy	zz (π)	Av	$\delta^1\text{H}^a$
Terthiophene (3T)					
H1	25.6	25.1	21.3 (-1.67)	24.0	7.5
H3	24.8	27.5	21.4 (-1.71)	24.5	7.0
H5	26.8	26.6	19.3 (-2.61)	24.2	7.3
H7	27.0	26.6	19.3 (-2.45)	24.3	7.2
Pentathienoacene (5TA)					
H1	26.0	25.0	20.3 (-2.33)	23.8	7.7
H3	25.7	26.9	19.5 (-3.11)	24.0	7.5
Quinoidal Terthiophene (Q3T)					
H1	30.7	24.0	23.7 (-0.26)	26.1	5.4
H3	30.1	23.4	24.2 (-0.08)	25.9	5.6
H5	27.3	24.1	22.6 (-0.62)	24.7	6.8
H7	28.7	24.1	21.1 (-0.67)	24.6	6.9
H9	28.8	24.1	20.9 (-0.72)	24.6	6.9
Quinoidal Pentathienoacene (Q5TA)					
H1	30.9	24.0	23.7 (-0.28)	26.2	5.3
H3	30.5	23.4	24.0 (-0.18)	26.0	5.5
H5	28.8	24.8	22.0 (-0.99)	25.2	6.3
Pentathiophene (5T)					
H1	25.7	25.0	21.2 (-1.69)	24.0	7.5
H3	24.8	27.5	21.3 (-1.72)	24.5	7.0
H5	26.9	26.5	19.2 (-2.62)	24.2	7.3
H7	27.1	26.6	19.2 (-2.48)	24.3	7.2
H9	27.4	26.6	19.1 (-2.41)	24.4	7.1
H11	27.4	26.6	19.1 (-2.65)	24.4	7.1
Nonathienoacene (9TA)					
H1	25.6	25.0	20.2 (-2.38)	23.6	7.9
H3	25.8	26.9	19.3 (-3.15)	24.0	7.5
Quinoidal Pentathiophene (Q5T)					
H1	30.7	23.9	23.6 (-0.28)	26.1	5.4
H3	30.2	23.4	24.2 (-0.10)	25.9	5.6
H5	27.5	24.1	22.6 (-0.64)	24.7	6.8
H7	28.7	24.1	21.0 (-0.73)	24.6	6.9
H9	28.9	24.2	20.7 (-0.79)	24.6	6.9
H11	29.0	24.0	20.6 (-0.86)	24.5	7.0
H13	29.0	24.1	20.6 (-0.86)	24.6	6.9
Quinoidal Nonathienoacene (Q9TA)					
H1	31.0	23.9	23.6 (-0.33)	26.1	5.4
H3	30.5	23.4	23.9 (-0.23)	25.9	5.6
H5	28.8	24.7	21.7 (-1.08)	25.1	6.4

^a Chemical shifts are referenced to thiophene values: $\sigma_{\text{Av}}(\text{H}) = 24.50$, $\delta^1\text{H} = 6.96$. ^b Contributions from π electrons to the zz component are given within parentheses. $\sigma_{\text{Av}} = (\sigma_{\text{xx}} + \sigma_{\text{yy}} + \sigma_{\text{zz}})/3$.

aromatic character of the quinoidal form as the size of the oligomer is enlarged. The same numbers illustrate the second important fact: the fused oligomers lose a larger fraction of aromaticity when adopting the quinoidal structure.

The difference in aromaticity between aromatic and quinoidal structures is better observed by comparing the proton magnetic shieldings (Table 2). The values calculated for the ^1H NMR shieldings of the **3T**, **5TA**, **5T**, and **9TA** oligomers are typical of aromatic compounds. For these oligomers, the deshielding attributable to the π -electrons is in general larger than 2 ppm, while for the quinoidal forms it is smaller than 1 ppm for the thiophene protons and almost negligible for the vinylene protons.

Proton magnetic shieldings can also be used to establish a direct comparison between nonfused and fused oligomers. For the aromatic trimers, protons H₁ of **3T** and **5TA** (see Scheme 1 for atom numbering) are in equivalent environ-

Table 3. Aromaticity Index HOMA of the Individual Thiophene Rings for Oligothiophenes and Oligothienoacenes

index HOMA	central ring	2 nd ring	terminal ring
terthiophene (3T)	0.709		0.724
pentathiophene (5T)	0.715	0.714	0.727
pentathiophene (5TA)	0.713	0.697	0.727
nonathienoacene (9TA)	0.714	0.714	0.730
quinoidal terthiophene (Q3T)	0.324		0.228
quinoidal pentathiophene (Q5T)	0.496	0.450	0.211
quinoidal pentathiophene (Q5TA)	0.335	0.305	0.137
quinoidal nonathienoacene (Q9TA)	0.519	0.478	0.207

ments, and, therefore, the differences in the zz component of the shielding tensor can be precisely associated with the differences in the corresponding ring currents. Accordingly, the values of 21.3 ppm for **3T** and 20.3 ppm for **5TA** show that the ring current is more intense in the terminal ring of the fused oligomer, as the deshielding produced for **5TA** (-2.33 ppm) is larger.

A similar analysis on H₁ protons of the aromatic pentamers **5T** and **9TA** shows that the reduction of the ^1H NMR shielding tensor ($\sigma_{\text{zz}} = 21.2$ and 20.2 ppm, respectively) is slightly larger than that of the corresponding trimers. This suggests that the intensity of the ring current increases with the size of the oligomer. The trend has been confirmed by extending the study to include also heptathiophene, though using the smaller 6-31G** basis set to calculate the shielding tensor. As shown in Table S1 in the Supporting Information, the computed numerical values are slightly different from those reported in Table 2 using the larger Dunning's basis sets, but the general features are kept. Calculations predict that the proton deshielding due to π electrons increases as the oligomer chain becomes longer. In particular, $\sigma_{\text{zz}}(\pi)$ takes values of -2.35, -2.36, and -2.44 ppm for the inner proton of the terminal ring of **3T**, **5T**, and **7T**, respectively. Furthermore, the deshielding slightly decreases in going from the central to the external thiophene rings, with the exception of the terminal rings for which the contribution to deshielding of the π -electrons is the largest.

For the quinoidal trimers **Q3T** and **Q5TA**, it is possible to compare the vinylene protons H₁ close to the sulfur atoms. Again, the deshielding attributed to the π electrons is larger for the fused oligomer (-0.28 ppm) than for the nonfused oligothiophene (-0.26 ppm). The remaining protons of **Q3T** and **Q5TA** present slightly different environments even in analogous positions, but all of them appear more deshielded in **Q5TA** (H₃: -0.18 ppm, H₅: -0.99 ppm) than in **Q3T** (H₃: -0.08 ppm, H₅: -0.62 ppm). In any case, the values of π -deshielding found for σ_{zz} of the vinylene protons are intermediate between those found for a nonaromatic quinoidal phenanthrene (-0.10 and -0.16 ppm) and those obtained for a more extended quinoidal system that possesses some aromatic character (-0.40 and -0.46 ppm).³⁷

As discussed for the aromatic oligomers, the quinoidal pentamers **Q5T** and **Q9TA** also present larger π -deshieldings than the equivalent trimers, even for the vinylene protons (see Table 2). It is important to note that this effect turns out to be more significant in the environment of the central

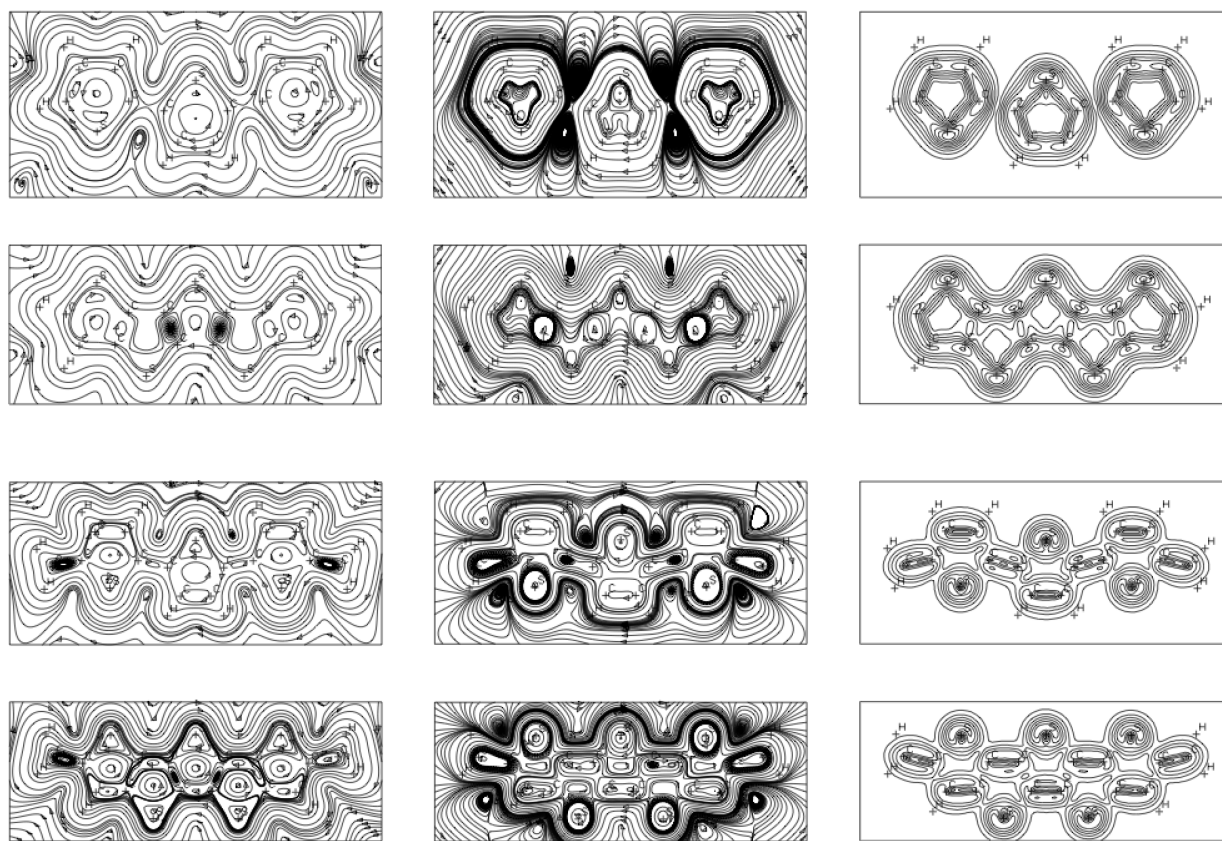


Figure 1. Streamlines of the total current density (left) and π -electron contributions to the current density (center) on a plane at 1.1 bohr above the molecular plane and contour levels for the modulus of the π current (right) for (top to bottom) **3T**, **5TA**, **Q3T**, and **Q5TA**. The maximum modulus (contour step) values are 0.069 (0.007), 0.075 (0.008), 0.033 (0.005) and 0.034 (0.005), respectively, in au.

ring, for which the changes are larger when the oligomer becomes longer. This suggests that the central part of the oligomer becomes more aromatic as the quinoidal chain lengthens. This partial aromatization is in agreement with the reduction in the CC bond length alternation (difference between the length of single and double bonds) calculated for the central ring in passing from **Q3T** (0.070 Å) to **Q5T** (0.047 Å) and with previous geometrical results obtained for quinoidal oligothiophenes end-capped with dicyanomethylene groups.^{38–40}

To facilitate comparison to available experimental data, we have also computed ^1H chemical shifts taking tetramethylsilane (TMS) as reference. In terthiophenes and similar derivatives it is experimentally observed that for protons in the central ring $\delta(\text{H})$ oscillates between 7.0 and 7.7 ppm, while for the central ring $\delta(\text{H}) = 7.0\text{--}7.2$ ppm.⁴¹ In the case of pentathienoacene, it has been determined that $\delta(\text{H}_1) = 7.4$ ppm and $\delta(\text{H}_3) = 7.3$ ppm. In addition, an increase of proton chemical shifts with the number of rings has been found in analogous compounds.⁴² A reasonable agreement is encountered between these experimental values and the calculated values reported in Table 2, which illustrates the quality of our theoretical data. Still, let us remark that our analysis is based on the π -contributions to the out-of-plane shielding. Such contribution is not available to experiment, but according to the classical picture is the one directly related to aromaticity.

Other criteria as, for instance, the Harmonic Oscillator Model of Aromaticity, HOMA,⁴³ (see Table 3) lead to similar conclusions in quantifying the aromaticity of the studied species. The HOMA index takes the value of 0 for a Kekulé structure of a typical aromatic system and the value of 1 for systems with all bond lengths equal to the optimal value as in benzene. We find that the HOMA indices calculated for the thiophene rings in the fused oligomers are larger than those obtained for the nonfused compounds and that they increase with the size of the oligomer. This suggests once more that oligothienoacenes are slightly more aromatic than nonfused oligothiophenes and that the degree of aromaticity increases with the oligomer length. It is also observed that while in the aromatic oligomers the largest indices are encountered for the terminal rings, in the quinoidal structures the highest HOMA index corresponds to the central ring. This correlates with the slight aromatization of the central part of the quinoidal structures inferred from π -deshielding values.

3.2. Current Density Maps. The representations of the current density induced by a uniform magnetic field applied along the positive z axis perpendicular to the molecular plane provide a direct visualization of the phenomenology of molecules in a magnetic field. By applying the RCM, it is possible to quantify the aromaticity of the molecule and the delocalization of the π -electrons through the modulus and the direction of the currents. Two different kinds of current

density maps have been used to this aim. The first type displays the streamlines of the current density with the corresponding modulus represented by contour curves. The second type uses arrows in the direction of the current, their length being locally proportional to the current density in that point. The second type of maps yields a less-detailed description, but it is enough to illustrate the essential features of the flow. The region examined in this study is approximately that of maximum of the π -density, 1.1 bohr above the plane of the molecule.⁴⁴ Diamagnetic currents are clockwise, while paramagnetic ones are in the opposite sense.

Figure 1 shows the streamlines of the total and π -current densities as well as the modulus of the π -current density for the four trimers under study. The streamlines for the total current density (left column in Figure 1) present common features in all systems: a diamagnetic flow runs around the molecular periphery and paramagnetic vortices appear on the ring centers, which is typical of planar conjugated cyclic molecules. The π -current density maps (central column in Figure 1) display different characteristics for each molecule. For the aromatic trimers, there exist strong diatropic ring currents, but their topologies are sensibly different depending on the structure of the oligomer. For fused **5TA**, an intense current is delocalized around the whole molecular perimeter, as it were a single cycle, in a way analogous to that found for naphthalene⁴⁵ or thieno[3,2-b]thiophene.⁴⁴ In contrast, for nonfused **3T**, the aromaticity of the thiophene ring prevails and distinct patterns of noninteracting diamagnetic currents localized on each thiophene ring are observed. For the quinoidal trimers, the localized circulation around the double CC bonds is worth noticing. The different regime of the π -current densities is best shown by the shape of the contour maps in Figure 1.

Figure 1 indicates that the intensities of the current densities are also different. The absolute maximum of the π -current density corresponds in all cases to islands of flow, each centered about a sulfur nucleus. Each circulation has the same diatropic sense as the peripheral ring current but a much smaller radius. The maximum modulus is different for each oligomer: 0.069 (**3T**), 0.075 (**5TA**), 0.033 (**Q3T**), and 0.034 au (**Q5TA**). The π -ring current densities (i.e., the global circulation of current delocalized around the whole molecular perimeter as in benzene) also show different features. In **5TA** the most intense π -ring current reaches a modulus as big as 0.043 au, while in **3T** the maximum values of the ring current intensity are 0.039 and 0.033 au for the terminal and central thiophene rings, respectively.

The intensity and the pattern of the ring currents change drastically for the quinoidal trimers (see Figure 1). A substantial reduction of intensity of the ring currents takes place with respect to the aromatic partners, the maximum values being 0.0080 au for **Q3T** and 0.0081 au for **Q5TA** (c.a. five times smaller than in their aromatic partners). The most distinctive feature observed for the quinoidal trimers is the diamagnetic π -current showing vortices and foci located in the regions of the formal double bonds. This result shows that double CC bonds prevail as the main π -entity in quinoidal oligomers and suggests that π electrons are more localized in these systems than in their aromatic partners.

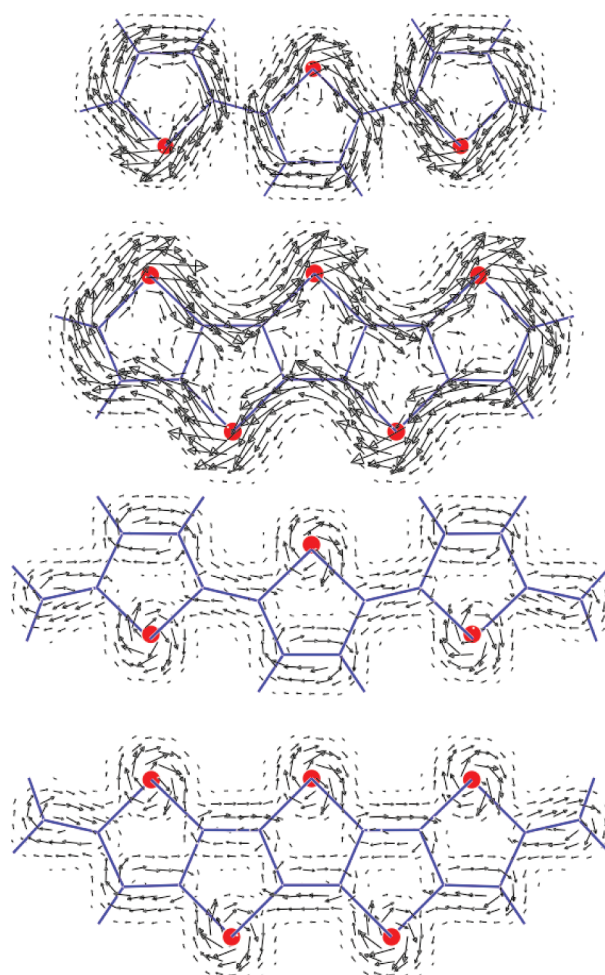


Figure 2. π -electron contribution to the current density on a plane at 1.1 bohr for (top to bottom) **3T**, **5TA**, **Q3T**, and **Q5TA**. The maximum modulus values are 0.069, 0.075, 0.033, and 0.034 au, respectively. The length of the arrows is normalized to the maximum modulus in benzene (0.080 au). Intensities lower than 0.004 au are omitted.

The intensity and direction of the currents can be simultaneously observed in the maps depicted in Figure 2. For the aromatic trimers, the ring currents described above are clearly seen, and it is straightforward to show that fused **5TA** is more aromatic than its nonfused counterpart **3T** since the current density is more intense in the former. The topology of the current density maps for the quinoidal trimers is very different from that for their aromatic partners. First, the π -currents are much less intense as it can be easily checked from inspection of the figure, where the arrows representing the density currents for the quinoidal systems **Q3T** and **Q5TA** are shorter than those for the aromatic systems **3T** and **5TA**. Second, the distribution of the currents is completely changed: the ring currents flowing around the molecular periphery of the quinoidal systems appear in Figure 2 as very short arrows—virtually points—which describe a weak annular diatropism. At any rate, the currents localized on sulfur atoms and double bonds clearly predominate, and local diamagnetic π vortices, typical of formal C=C double bonds, are observed. Thus, the π electrons are rather localized as in conjugated nonaromatic polyenes.

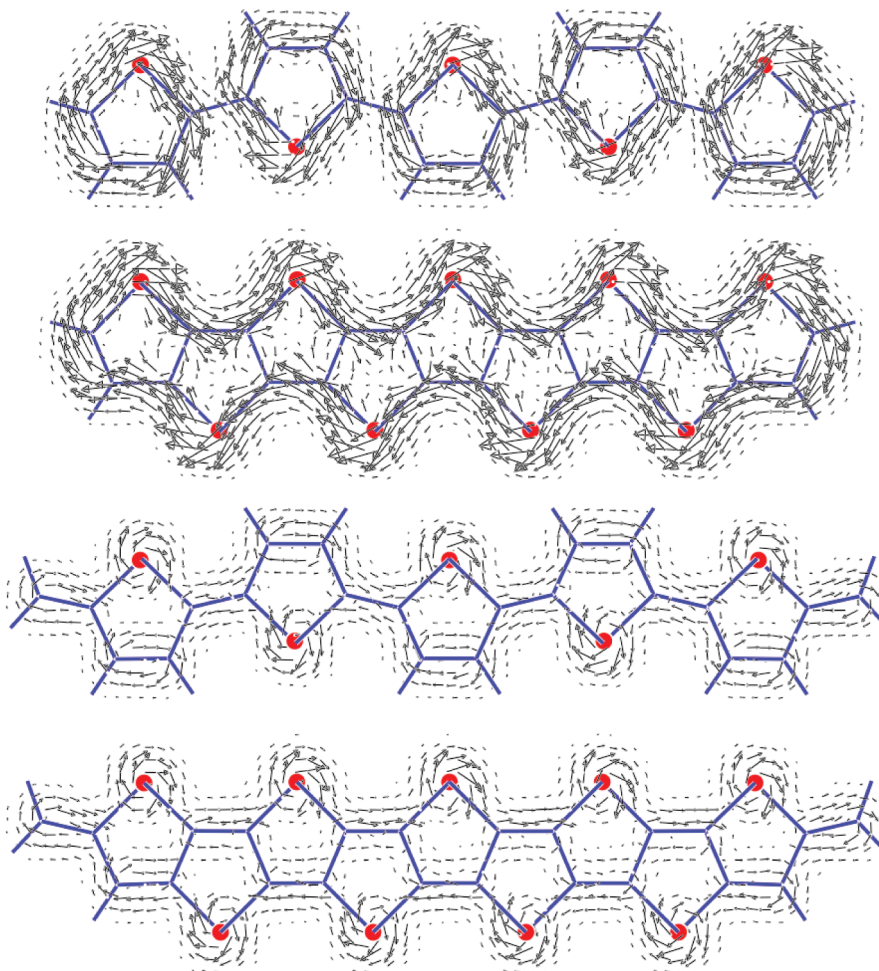


Figure 3. π -electron contribution to the current density on a plane at 1.1 bohr above the molecular plane for (top to bottom) **5T**, **Q5T**, and **Q9TA**. The maximum modulus values are 0.069, 0.075, 0.033, and 0.036 au, respectively. The length of the arrows is normalized to the maximum modulus in benzene (0.080 au). Intensities lower than 0.004 au are omitted.

By close inspection of the two set of maps (Figure 1 and 2) for the quinoidal trimers, one can observe a current streamline flowing over all the double bonds in the thiophene rings, which would imply a small degree of delocalization. Since this current is somewhat more intense in the case of the fused oligomer, the delocalization effects are slightly more sizable for the fused oligomer **Q5TA** than for the nonfused terthiophene **Q3T**. This fact is in agreement with the larger π -contribution to proton deshielding ($\sigma_{zz}(\pi)$) in **Q5TA** than in **Q3T** (see Table 2) mentioned above.

There is no major change in the intensity of the ring currents for the aromatic pentamers **5T** and **9TA** compared with their equivalent trimers. However, significant differences are found for quinoidal oligomers, for which the ring currents have intensities of 0.0083 (**Q5T**) and 0.0088 au (**Q9TA**). The fused **Q9TA** pentamer therefore shows ring currents almost 10% more intense than the corresponding **Q5TA** trimer. The streamlines and modulus maps (Figure S3) present characteristics which are completely similar to those discussed for the corresponding trimers, i.e., peripheral ring currents around the whole aromatic structure for fused **9TA**, in-ring-restricted currents for the aromatic nonfused **5T**, and circulation involving the ethylenic bonds for the quinoidal oligomers **Q5T** and **Q9TA**. The arrows maps displayed in Figure 3 illustrate an important feature that is not detectable

in previous maps. For **Q9TA**—and for longer thienoacenes—it is observed that the outward current in the CC double bonds is much more intense than the return current inside the rings, indicating a larger delocalization of the π -electronic density. In fact, the diamagnetic perimeter circulation grows going from **Q5T** (in which vortices about the double bonds are clearly discernible) to **Q9TA** (in which no closed current loops are found in the region of internal formal double bonds). This effect is only observable for the central rings of fused **Q9TA**. We could not detect it either in the nonfused **Q5T** or the quinoidal trimers, which suggests that the delocalization of the ethylenic bonds requires a minimum size of the oligomer to take place. In **Q9TA** the current density about double bonds cannot form closed loops. On the other hand, it gives rise to continuous π -ring current flowing all over the carbon skeleton visible in the map of **Q9TA** as a peripheral delocalized stream more intense than in the other quinoidal oligomers.

Summarizing, the stronger intensity of the peripheral ring π -current, the absence of closed current loops about the formal double bonds, and the consequent weakening of the return currents indicate that **Q9TA** possesses a higher degree of π -conjugation than other quinoidal oligomers. This is confirmed by the numerical estimates of the π -contribution to the out-of-plane component of proton magnetic shieldings.

4. Conclusions

By means of magnetic criteria, we have evaluated the aromaticity of a series of thiophene-based oligomers with both fused/nonfused and aromatic/quinoidal structures. Our theoretical analysis uses a comparison of results obtained from calculations of magnetic susceptibility, ^1H NMR shieldings, and ring currents. All the considered systems, either aromatic or quinoidal, exhibit large and negative values of the magnetic susceptibility and, in particular, of the χ_{zz} component. The deshielding $\sigma_{zz}(\pi)$ contribution to the proton shielding tensor clearly indicates that fused oligothienoacenes are slightly more aromatic than nonfused α -oligothiophenes. It also implies that the degree of aromaticity increases with the oligomer length and going from inner to outer thiophene rings along the chain. π -deshielding values also predict a weak aromatization of the central part of the conjugated chain for quinoidal oligomers increasing with the oligomer size. These trends are also supported by the values obtained for the aromaticity HOMA index. The conversion from aromatic to quinoidal structures obviously implies a loss of aromaticity, which is larger in the case of the thienoacenes.

The π -currents induced by a uniform magnetic field applied perpendicular to the molecular plane display a drastically different topology depending on the structure of the oligomer. Fused oligothienoacenes behave as single cycles and show an intense current flowing around the whole molecular perimeter. In contrast, the aromaticity of the thiophene ring prevails for nonfused α -oligothiophenes which present diamagnetic currents around each thiophene ring. For the quinoidal oligomers, local diamagnetic π vortices, typical of formal CC double bonds, are observed, indicating that the π electrons are rather localized as in conjugated, nonaromatic polyenes. However, the electronic circulation around the ethylenic bonds in the quinoidal nonathienoacene (**Q9TA**) tends to delocalize all over the carbon skeleton giving the molecule some aromatic character. The effect is more pronounced for the central rings and is not observed for the trimer **Q5TA**, thus suggesting that the delocalization of the ethylenic bonds requires a minimum size of the oligomer to be effective. A progressive gain of aromatic character is therefore expected on increasing the length of fused quinoidal systems. This effect has been already predicted for quinoidal benzene-fused systems.³⁷

Acknowledgment. This work has been supported by the Spanish Ministry of Education and Science (MEC; projects CSD2007-00010, CTQ2006-14987-C02-02, CTQ2007-67143-C02-01/BQU, and CT2009-08790), the Generalitat Valenciana (ACOMP07/163, GV/2007/093, and GVAINF 2007-051), and European FEDER funds. J.A. acknowledges the MEC for a FPI doctoral grant.

Supporting Information Available: CTOCD-DZ2/6-31G** perpendicular component of ^1H NMR shieldings (σ_{zz}) and contributions from π electrons for α,α' -linked oligothiophenes containing three, five, and seven rings, streamlines and modulus of the π current for **5T**, **9TA**, **Q5T**, and **Q9TA**, and a sensibly enlarged version of Figure 1 in order to facilitate its interpretation. This material is available free of charge via the Internet at <http://pubs.acs.org>.

References

- (1) von Ragué Schleyer, P. *Chem. Rev.* **2001**, *101*, 1115–1117.
- (2) For a recent review on organic materials for molecular electronics see the monographic issues: (a) Organic Electronics and Optoelectronics. *Chem. Rev.* **2007**, *107* (4), (b) Organic Electronics. *Chem. Mater.* **2004**, *16*, (23).
- (3) (a) *Molecular Nanoelectronics*; Reed, M. A., Lee, T., Eds.; American Scientific Publishers: Stevenson Ranch, CA, 2003. (b) Tour, J. M. *Molecular Electronics: Commercial Insights, Chemistry, Devices, Architecture and Programming*; World Scientific: 2003. (c) Petty, M. *Molecular Electronics: From Principles to Practice*; John Wiley & Sons: 2008.
- (4) Roncali, J. *Chem. Rev.* **1997**, *97*, 173–205; **1992**, *92*, 711–738.
- (5) Müllen, K.; Wegner, G. *Electronic materials: The oligomer Approach*; Wiley-VCH: 1998.
- (6) Fichou, D. *Handbook of oligo- and Polythiophenes*; Wiley-VCH: Weinheim, 1999.
- (7) (a) Facchetti, A.; Yoon, M. H.; Stern, C. L.; Hutchinson, G. R.; Ratner, M. A.; Marks, T. J. *J. Am. Chem. Soc.* **2004**, *126*, 13480–13501. (b) Facchetti, A.; Mushrush, M.; Yoon, M. H.; Hutchinson, G. R.; Ratner, M. A.; Marks, T. J. *J. Am. Chem. Soc.* **2004**, *126*, 13859–13874. (c) Yoon, M. H.; di Bennedetto, S. A.; Russell, M. T.; Facchetti, A.; Marks, T. J. *Chem. Mater.* **2007**, *19*, 4864–4881.
- (8) Peart, P. A.; Repka, L. M.; Tovar, J. D. *Eur. J. Org. Chem.* **2008**, 2193–2206.
- (9) Mitschke, U.; Bäuerle, P. *J. Mater. Chem.* **2000**, *10*, 1471–1507.
- (10) Coakley, K. M.; McGehee, M. D. *Chem. Mater.* **2004**, *16*, 4533–4542.
- (11) Murphy, A. R.; Fréchet, J. M. J. *Chem. Rev.* **2007**, *107*, 1066–1096.
- (12) Dimitrakopoulos, C. D.; Malenfant, P. R. L. *Adv. Mater.* **2002**, *14*, 99–117.
- (13) Bao, Z.; Rogers, J. A.; Katz, H. E. *J. Mater. Chem.* **1999**, *9*, 1895–1904.
- (14) Katz, H. E. *Chem. Mater.* **2004**, *16*, 4748–4756.
- (15) *Handbook of Conducting Polymers*, 2nd ed.; Skotheim, T. A., Elsenbaumer, R. L., Reynolds J. R., Eds.; Marcel Dekker: New York, 1998.
- (16) (a) Brédas, J.-L.; Chance, R. R.; Silbey, R. *Phys. Rev. B* **1982**, *26*, 5843. (b) Brédas, J.-L.; Street, G. B. *Acc. Chem. Res.* **1985**, *18*, 309–315.
- (17) (a) Kertesz, M.; Lee, Y.-S. *J. Phys. Chem.* **1987**, *91*, 2690–2692. (b) Lee, Y.-S.; Kertesz, M. *J. Chem. Phys.* **1988**, *88*, 2609–2617.
- (18) Schulze, K.; Riede, M.; Brier, E.; Reinold, E.; Bäuerle, P.; Leo, K. *J. Appl. Phys.* **2008**, *104*, 074511.
- (19) *Handbook of Thiophene-Based Materials: Applications in Organic Electronics and Photonics*; Perepichka, I. F., Perepichka, D. F., Eds.; Wiley: Weinheim, 2009.
- (20) (a) Zhang, X.; Côte, A. P.; Matzger, A. J. *J. Am. Chem. Soc.* **2005**, *127*, 10502–10503. (b) Okamoto, T.; Kudoh, K.; Wakamiya, A.; Yamaguchi, S. *Chem.—Eur. J.* **2007**, *13*, 548–556.
- (21) (a) Xiao, K.; Liu, Y.; Qi, T.; Zhang, W.; Wang, F.; Gao, J.; Qiu, W.; Ma, Y.; Cui, G.; Chen, S.; Zhan, X.; Yu, G.; Qin,

- J.; Hu, W.; Zhu, D. *J. Am. Chem. Soc.* **2005**, *127*, 13281–13286. (b) Gao, P.; Beckmann, D.; Tsao, H. N.; Feng, X.; Enkelmann, V.; Pisula, W.; Müllen, K. *Adv. Mater.* **2009**, *21*, 213–216.
- (22) (a) Osuma, R. M.; Zhang, X.; Matzger, A. J.; Hernández, V.; López-Navarrete, J. T. *J. Phys. Chem. A.* **2006**, *110*, 5058–5065. (b) Aragó, J.; Viruela, P. M.; Ortí, E. *J. Mol. Struct., Theochem*, in press.
- (23) Pauling, L. *J. Chem. Phys.* **1936**, *4*, 673–677.
- (24) Lonsdale, K. *Proc. R. Soc. (London)* **1937**, *A159*, 149–170.
- (25) London, F. *J. Phys. Radium* **1937**, *8*, 397. 7ème Série.
- (26) Lazzeretti, P. in *Progress in Nuclear Magnetic Resonance Spectroscopy*; Emsley, J. W., Feeney, J., Sutcliffe, L. H., Eds.; Elsevier: Amsterdam, 2000; Vol. 36, p 188.
- (27) Gomes, J. A. N. F.; Mallion, R. B. *Chem. Rev.* **2001**, *101*, 1349–1383.
- (28) Lazzeretti, P. *Phys. Chem. Chem. Phys.* **2004**, *6*, 217–223.
- (29) Zanasi, R. *J. Chem. Phys.* **1996**, *105*, 1460–1469.
- (30) Lazzeretti, P.; Malagoli, M.; Zanasi, R. Technical Report on Project “Sistemi informatici e calcolo parallelo”; Research Report 1/67, CNR; 1991.
- (31) Dunning, T. H., Jr. *J. Chem. Phys.* **1989**, *90*, 1007–1023.
- (32) Woon, D.; Dunning, T. H., Jr. *J. Chem. Phys.* **1995**, *103*, 4572–4585.
- (33) Peterson, K. A.; Dunning, T. H., Jr. *J. Chem. Phys.* **2002**, *117*, 10548–10560.
- (34) Becke, A.D. *J. Chem. Phys.* **1993**, *98*, 1372–1377.
- (35) Franci, M. M.; Pietro, W. J.; Hehre, W. J.; Binkley, J. S.; Gordon, M. S.; Defrees, D. J.; Pople, J. A. *J. Chem. Phys.* **1982**, *77*, 3654–3665.
- (36) Frisch, M. J.; Trucks, G. W.; Schlegel, H. B.; Scuseria, G. E.; Robb, M. A.; Cheeseman, J. R.; Montgomery, J. A., Jr.; Vreven, T.; Kudin, K. N.; Burant, J. C.; Millam, J. M.; Iyengar, S. S.; Tomasi, J.; Barone, V.; Mennucci, B.; Cossi, M.; Scalmani, G.; Rega, N.; Petersson, G. A.; Nakatsuji, H.; Hada, M.; Ehara, M.; Toyota, K.; Fukuda, R.; Hasegawa, J.; Ishida, M.; Nakajima, T.; Honda, Y.; Kitao, O.; Nakai, H.; Klene, M.; Li, X.; Knox, J. E.; Hratchian, H. P.; Cross, J. B.; Adamo, C.; Jaramillo, J.; Gomperts, R.; Stratmann, R. E.; Yazyev, O.; Austin, A. J.; Cammi, R.; Pomelli, C.; Ochterski, J. W.; Ayala, P. Y.; Morokuma, K.; Voth, G. A.; Salvador, P.; Dannenberg, J. J.; Zakrzewski, V. G.; Dapprich, S.; Daniels, A. D.; Strain, M. C.; Farkas, O.; Malick, D. K.; Rabuck, A. D.; Raghavachari, K.; Foresman, J. B.; Ortiz, J. V.; Cui, Q.; Baboul, A. G.; Clifford, S.; Cioslowski, J.; Stefanov, B. B.; Liu, G.; Liashenko, A.; Piskorz, P.; Komaromi, I.; Martin, R. L.; Fox, D. J.; Keith, T.; Al-Laham, M. A.; Peng, C. Y.; Nanayakkara, A.; Challacombe, M.; Gill, P. M. W.; Johnson, B.; Chen, W.; Wong, M. W.; Gonzalez, C.; Pople, J. A. *GAUSSIAN03*; Gaussian Inc.: Wallingford, CT, 2004.
- (37) Faglioni, F.; Ligabue, A.; Pelloni, S.; Soncini, A.; Viglione, R. G.; Ferraro, M. B.; Zanasi, R.; Lazzeretti, P. *Org. Lett.* **2005**, *7*, 3457–3460.
- (38) (a) Casado, J.; Miller, L. L.; Mann, K. R.; Pappnus, T. M.; Higuchi, H.; Ortí, E.; Milián, B.; Pou-Amérigo, R.; Hernández, V.; López-Navarrete, J. T. *J. Am. Chem. Soc.* **2002**, *124*, 12380–12388. (b) Casado, J.; Pappnus, T. M.; Mann, K. R.; Ortí, E.; Viruela, P. M.; Milián, B.; Hernández, V.; López Navarrete, J. T. *ChemPhysChem.* **2004**, *5*, 529–539.
- (39) Milián, B.; Ortí, E.; Hernández, V.; López Navarrete, J. T.; Otsubo, T. *J. Phys. Chem. B* **2003**, *107*, 12175–12183.
- (40) (a) Ortiz, R. P.; Casado, J.; Hernández, V.; López Navarrete, J. T.; Ortí, E.; Viruela, P. M.; Milián, B.; Hotta, S.; Zotti, G.; Zecchin, S.; Vercelli, B. *Adv. Funct. Mater.* **2006**, *16*, 531–536. (b) Ponce Ortiz, R.; Casado, J.; Hernández, V.; López Navarrete, J. T.; Viruela, P. M.; Ortí, E.; Takimiya, K.; Otsubo, T. *Angew. Chem., Int. Ed.* **2007**, *46*, 9057–9061.
- (41) (a) Merz, A.; Ellinger, F. *Synthesis* **1991**, 462–464. (b) Henze, O.; Feast, J.; Gardeben, F.; Jonkheijm, P.; Lazzaroni, R.; Leclère, P.; Meijer, E. W.; Schenning, A. P. *J. Am. Chem. Soc.* **2006**, *128*, 5923–5929. (c) Yoon, M.-H.; Facchetti, A.; Stern, C. E.; Marks, T. J. *J. Am. Chem. Soc.* **2006**, *128*, 5792–5801.
- (42) Sato, N.; Mazaki, Y.; Kobayashi, K.; Kobayashi, T. *J. Chem. Soc., Perkin Trans. 2* **1992**, 765–770.
- (43) Krygowski, T. M.; Cyranski, M. K. *Chem. Rev.* **2001**, *101*, 1385–1419.
- (44) Cuesta, I. G.; Soriano, R.; Sánchez de Merás, A.; Lazzeretti, P. *Mol. Phys.* **2005**, *103*, 789–801.
- (45) Cuesta, I. G.; Sánchez de Merás, A.; Pelloni, S.; Lazzeretti, P. *J. Comput. Chem.* **2009**, *30*, 551–564.

CT900127M